Research in Astronomy and Astrophysics, 22:055018 (11pp), 2022 May https://doi.org/10.1088/1674-4527/ac630f

Crust Cooling of Soft X-Ray Transients—the Uncertainties of Shallow Heating

Xiang-Yang Lu[1,2], Guo-Liang Lü[1,2], He-Lei Liu[1,2], Chun-Hua Zhu[1,2], and Zhao-Jun Wang[1,2]
[1] School of Physical Science and Technology, Xinjiang University, Urumqi 830046, China; heleiliu@xju.edu.cn
[2] Center for Theoretical Physics, Xinjiang University, Urumqi 830046, China
Received 2021 November 24; revised 2022 March 20; accepted 2022 March 28; published 2022 April 29

Abstract

Crust cooling of soft X-ray transients has been observed after outbursts, but an additional shallow heating during accretion in outburst is needed to explain the quiescent light curve. However, shallow heating is significantly different between sources and even within one source between different outbursts, and the source of shallow heat is as yet unknown. Using the open source code "dStar" which solves the fully general relativistic heat diffusion equation for the crust, we investigate the effect of magnitude and depth of shallow heating on crust cooling and find that some exceptional sources (Swift J174805.3-244637, MAXI J0556-332 during outburst II and GRO J1750-27) in which shallow heating may be inactive could be explained by a deeper shallow heating mechanism. We compare our results with those from previous works and find that the shallow heating is model dependent. In addition, the effects of mass and radius of a neutron star on shallow heating are studied, and it is shown that the more compact the star, the less shallow heating will be needed to fit the crust cooling light curves.

Key words: stars: neutron – X-rays: binaries – stars: individual (GRO J1750-27) – X-rays: bursts

1. Introduction

Neutron stars in low-mass X-ray binaries (LMXBs) accrete matter from their companion, where the companion is typically a sub-solar star. Most of the systems are called soft X-ray transients (SXTs), and they do not accrete persistently but rather sporadically (Wijnands et al. 2017; Potekhin & Chabrier 2021). During outburst, matter accretes onto the neutron star surface via Roche-lobe overflow. The neutron star crust is heated up by the compression of accreted matter through a series of nuclear reactions which include electron capture, neutron emission and pycnonuclear reactions with the release of $\sim$1–2 MeV of energy per accreted nucleon (Haensel & Zdunik 1990, 2003, 2008). This process is referred to as "deep crustal heating" because most energy is produced in the pycnonuclear reactions which occur in the layers with densities of $10^{12\text{–}13}\,\mathrm{g\,cm^{-3}}$ (Brown et al. 1998). The typical outburst luminosity is in the range $10^{36\text{–}39}\,\mathrm{erg\,s^{-1}}$ for a relatively high accretion rate. It can last from weeks to months for ordinary transients, and in some rare cases (quasi-persistent transients) these outbursts can last years to decades. During the quiescent state where little accretion occurs, resulting in X-ray luminosities $<10^{34}\,\mathrm{erg\,s^{-1}}$, it can last years to decades. The observed quiescent luminosity will depend on the time-averaged accretion rate $\langle \dot{M} \rangle$ and properties of the neutron star. Therefore, studying the quiescent luminosity of transient accreting neutron stars provides a new avenue to understand the properties of dense matter in neutron star interiors (Yakovlev et al. 2003; Han & Steiner 2017; Matsuo & Liu 2018; Liu et al. 2021a). Once the crust of a neutron star is heated out of thermal equilibrium with the core during outburst, the crust will cool during quiescent phases. The crust cooling evolution of SXTs allows us to understand the thermal properties of a neutron star crust (Brown & Cumming 2009; Deibel et al. 2015; Parikh et al. 2020; Wijngaarden et al. 2020; Beznogov et al. 2021; Shchechilin et al. 2021; Liu et al. 2021b; Potekhin & Chabrier 2021).

The cooling of a neutron star crust has been observed from the quasi-persistent transient KS 1731-260 for the first time (Rutledge et al. 2002; Cackett et al. 2006). So far, there have been monitored crust coolings after accretion outbursts for 10 sources (Wijnands et al. 2017). An additional unknown heat in the outer layers of crust is needed to model these observed crust coolings. Fits to the light curve of MXB 1659-26 and KS 1731-260 consistently suggest that $\sim$1 MeV per accreted nucleon shallow heating at depth $10^{8\text{–}9}\,\mathrm{g\,cm^{-3}}$ is needed (Brown & Cumming 2009; Merritt et al. 2016; Ootes et al. 2016). Models of the quiescent light curve of Aql X-1 required the shallow heat of 2.3–9.2 MeV per accreted nucleon at a depth of $\sim 10^{10}\,\mathrm{g\,cm^{-3}}$ (Degenaar et al. 2019). The light curve of the hottest transient MAXI J0556-332 after outburst I required an additional heat source of 6–17 MeV per accreted nucleon at density $\sim 5.3 \times 10^9\,\mathrm{g\,cm^{-3}}$ (Deibel et al. 2015; Parikh et al. 2017a). However, the shallow heating mechanism was not active during its outbursts II and III (Parikh et al. 2017a). Although the magnitude and depth of shallow heating vary between the different outbursts and sources, its physical origin

Table 1
The Magnitude (Q_{sh}) and Depth (ρ_{sh}) of Shallow Heat Source Deposited in the Crust of Accreting Neutron Stars, as Needed by Cooling Simulations to Satisfy the Observational Data

SXT	Q_{sh}(MeV/u)	ρ_{sh} (g cm^{-3})	Reference
MXB 1659-29	0.4–2.0	1×10^8–0.9×10^{10}	Brown & Cumming (2009); Parikh et al. (2019)
	0.5–3.6	1×10^8–1.0×10^{10}	Turlione et al. (2015); Parikh et al. (2019)
KS 1731-260	1.38 ± 0.18	5×10^9	Merritt et al. (2016)
XTE J1701-462	0.17	2.2×10^{10}	Turlione et al. (2015)
EXO 0748-676	0.35–1.8	4.6×10^8	Degenaar et al. (2014)
Aql X-1	0.9–3.7	4×10^8–3.6×10^{10}	Waterhouse et al. (2016); Ootes et al. (2018)
	2.3–9.2	4×10^8–3.4×10^{10}	Degenaar et al. (2019)
IGR J17480-2446	1	4×10^8	Degenaar et al. (2013); Ootes et al. (2019)
	3.8	4.3×10^{11}	Turlione et al. (2015)
MAXI J0556-332	6–17	1.2×10^{10}	Deibel et al. (2015); Parikh et al. (2017a)
	2.2 ± 0.7 (0)	3.4×10^{10}	Parikh et al. (2017a)
	0.33 ± 0.03	1.6×10^9	Parikh et al. (2017a)
HETE J1900.1-2455	0–3	4×10^8	Degenaar et al. (2017)
1RXS J180408.9-342058	0.9	2.9×10^8	Parikh et al. (2018)
Swift J174805.3-244637	1.4	3.6×10^9	Degenaar et al. (2015)

is as yet unknown. As the heat is deposited at a shallower depth (10^{8-10} g cm^{-3}) in the neutron star crust than the deep crustal heating (10^{12-13} g cm^{-3}), it is referred to as the shallow heating mechanism. We summarize both the magnitude and depth of shallow heat which are needed during the crustal cooling simulations in Table 1.

There have been many works to study the shallow heating mechanism. As shallow heat amounts to about 1–2 MeV per accreted nucleon in most cases (MAXI J0556-332 and Aql X-1 are exceptions), part of this shallow heating could be explained by the envelope composition (Ootes et al. 2018) and uncertainties in the accretion rate (Degenaar et al. 2014; Turlione et al. 2015; Ootes et al. 2016). Chamel et al. (2020) estimated the maximum possible amount of heat that can be deposited in the outer crust of accreting neutron stars due to electron captures and pycnonuclear reactions with use of the existing experimental nuclear data. The upper limits still cannot explain the quiescent light curve of Aql X-1 and MAXI J0556-332 which need a large amount of shallow heat. It is worth mentioning that recently Page et al. (2022) proposed a new "hyperburst" in the MAXI J0556-332 neutron star before the end of its first outburst, and such a deep explosion could provide an excellent fit to the cooling data. However, it is difficult to witness another one in SXTs. The origin of the shallow heat source is still not fully understood.

On the other hand, in some cases (Swift J174805.3-244637, Degenaar et al. 2015, MAXI J0556-332 during outburst II, Parikh et al. 2017a, GRO J1750-27, Rouco Escorial et al. 2019), shallow heating was not found to be required in the crust cooling simulations. If a shallow heat source existed in these sources, it should be inactive. One may wonder: what are the conditions under which shallow heating was inactive in the accreting neutron star crust? It is necessary for us to investigate both the magnitude and depth of shallow heating during outburst that affect the shape of the cooling light curve. Besides, the different crust cooling models and the input parameters may lead to uncertainties in shallow heating. We will provide some discussion about it in this work.

The paper is organized as follows. In Section 2, we outline our model of crust cooling with use of the code dStar. In Section 3, we investigate the effect of magnitude and depth of shallow heating on crust cooling. In Section 4, we study the uncertainties of shallow heating from the models and the free parameters such as mass and radius. Finally, Section 5 is devoted to our conclusions.

2. Model

To analyze the effect of magnitude and depth of shallow heating on the crustal cooling light curves, we simulate the thermal evolution of a neutron star crust using the thermal evolution code dStar (Brown 2015), which solves the fully general relativistic heat diffusion equations

$$\frac{\partial}{\partial t}(Te^{\phi/c^2}) = e^{2\phi/c^2}\frac{\epsilon_{\rm nuc} - \epsilon_\nu}{C} - \frac{1}{4\pi r^2 \rho C(1+z)}\frac{\partial}{\partial r}(Le^{2\phi/c^2}), \tag{1}$$

$$Le^{2\phi/c^2} = -\frac{4\pi r^2 K e^{\phi/c^2}}{1+z}\frac{\partial}{\partial r}(Te^{\phi/c^2}), \tag{2}$$

where $\epsilon_{\rm nuc}$ and ϵ_ν represent nuclear heating and neutrino emissivity, respectively. C and K denote specific heat and thermal conductivity, respectively. $1+z = [1 - 2GM/(rc^2)]^{-1/2}$ is the gravitational redshift factor. The detailed microphysics of the

Table 2
The Fitting Parameters for the Crustal Cooling Simulations of Eight SXTs with use of dStar

SXT	M ($M_\odot$)	R (km)	$\dot{M}$ ($\times\ 10^{17}$g s^{-1})	t_{acc} (yr)	T_c ($\times\ 10^7$ K)	Q_{imp}	Q_{sh} (MeV/u)	log p_{sh} (ρ_{sh}) (erg cm^{-3} (g cm^{-3}))
MXB 1659-29								
Outburst I	1.6	12	1	2.5	2.9	2.6	0.85	27.0 (2.1×10^9)
Outburst II	1.6	12	0.32	1.7	2.9	2.6	1.1	26.6 (1.4×10^9)
MAXI J0556-332								
Outburst I	1.5	11	10	1.3	12	1	6.1	28.1 (1.4×10^{10})
Outburst II	1.5	11	5.5	0.17	21	1	8.3	28.3 (2.1×10^{10})
Outburst III	1.5	11	0.7	0.25	11	1	1.58	28.2 (1.7×10^{10})
KS 1731-260	1.4	10	1	12.5	5.8	4.4	0.61	27.6 (5.7×10^9)
XTE J1701-462	1.6	12	11.5	1.6	10	7	0.22	28.1 (1.6×10^{10})
EXO 0748-676	1.6	12	0.3	24	13.5	1	1.8	26.6 (9.9×10^8)
IGR J17480-2446	1.6	12	2	0.17	6.32	7	0.83	27.2 (2.9×10^9)
Swift J174805.3-244637	1.4	10	1	0.15	10.2	1	1	27.9 (9.8×10^9)
Aql X-1	1.6	11	2	0.17	8	1	8.3	28.6 (3.5×10^{10})

crust follows Brown & Cumming (2009) and the parameters of the cooling model are referenced from Deibel et al. (2015).

As shown in Table 1, shallow heating is different between sources and even within one source between different outbursts. Different models (“NSCool”, Page 2016, “dStar”, Brown 2015) are adopted to fit the crust cooling light curves, and we choose eight sources from Table 1 to simulate the crust cooling with use of dStar. For consistency in our dStar modeling, the values of the neutron star mass and radius, the initial core temperature of neutron star (T_c) and the impurity factor of the crust (Q_{imp}) follow the previous works. The column depth of light elements is fixed at $y = 10^8$ g cm^{-2}. The magnitude (Q_{sh}) and depth (ρ_{sh}) of shallow heating were model fit parameters. We change the magnitude and depth of shallow heating artificially to fit the observational data. Our fitting parameters can be found in Table 2.

3. The Effect of Magnitude and Depth of Shallow Heating on Crust Cooling

From the above section, we have modeled the crust cooling curves of eight sources (the crustal cooling of MXB 1659-29 and MAXI J0556-332 after multiple outbursts is also modeled) with use of dStar. As the magnitude and depth of shallow heating are different between sources and even within one source between different outbursts, we will investigate the effect of magnitude and depth of shallow heating on the cooling curves in this section.

3.1. The Effect of Magnitude of Shallow Heating on Crust Cooling Curves

Here we use a fixed set of conditions as given in Table 2 and explore the impact of changing magnitude of shallow heating on the crustal cooling light curves, see Figure 1. Note that a large amount of shallow heat makes a hot crust. In the case $Q_{sh} = 0$, the crust is heated by deep crustal heating only (the purple lines). As the accretion time is long for MXB 1659-29 during outburst I (2.5 yr), XTE J1701-462 (1.6 yr) and KS 1731-260 (12.5 yr), the crust is obviously heated out of the core temperature. However, the crust is heated out of the core temperature slightly because of the short accretion time for Swift J17480.5-244637 (~0.15 yr), which is why the light curves are different at the case $Q_{sh} = 0$. Besides accretion time, the accretion rate also affects the light curves a lot. For EXO 0748-676, the accretion time is ~24 yr; as its accretion rate is low, the simulated light curve is almost straight in the case $Q_{sh} = 0$. With increasing Q_{sh} of each source, the temperature at the top of the crust will increase.

From our simulations with different sources, we can conclude that even a small amount of shallow heat can increase the crust temperature (e.g., XTE J1701-462, IGR J17480-2446, MXB 1659-29, KS 1731-260). However, for Aql X-1, the crust is difficult to heat with increasing Q_{sh}. This is because the shallow heat is in a deeper layer in its crust.

3.2. The Effect of Depth of Shallow Heating on Crust Cooling Curves

Similarly, with use of the fitting parameters of eight sources in Table 2, by changing the depth of the shallow heat source, we investigated the effect of depth of shallow heat on the cooling curves. In Figure 2 we display the crust cooling curves with different depth (log p) of shallow heat. The deeper the shallow heat source is, the lower the crust temperature, and the longer time before crust cooling starts. As the depth of shallow heat source decreases, the crust temperature increases, and there is a shorter time before crust cooling begins. It is interesting to note that there is a large uncertainty in the depth

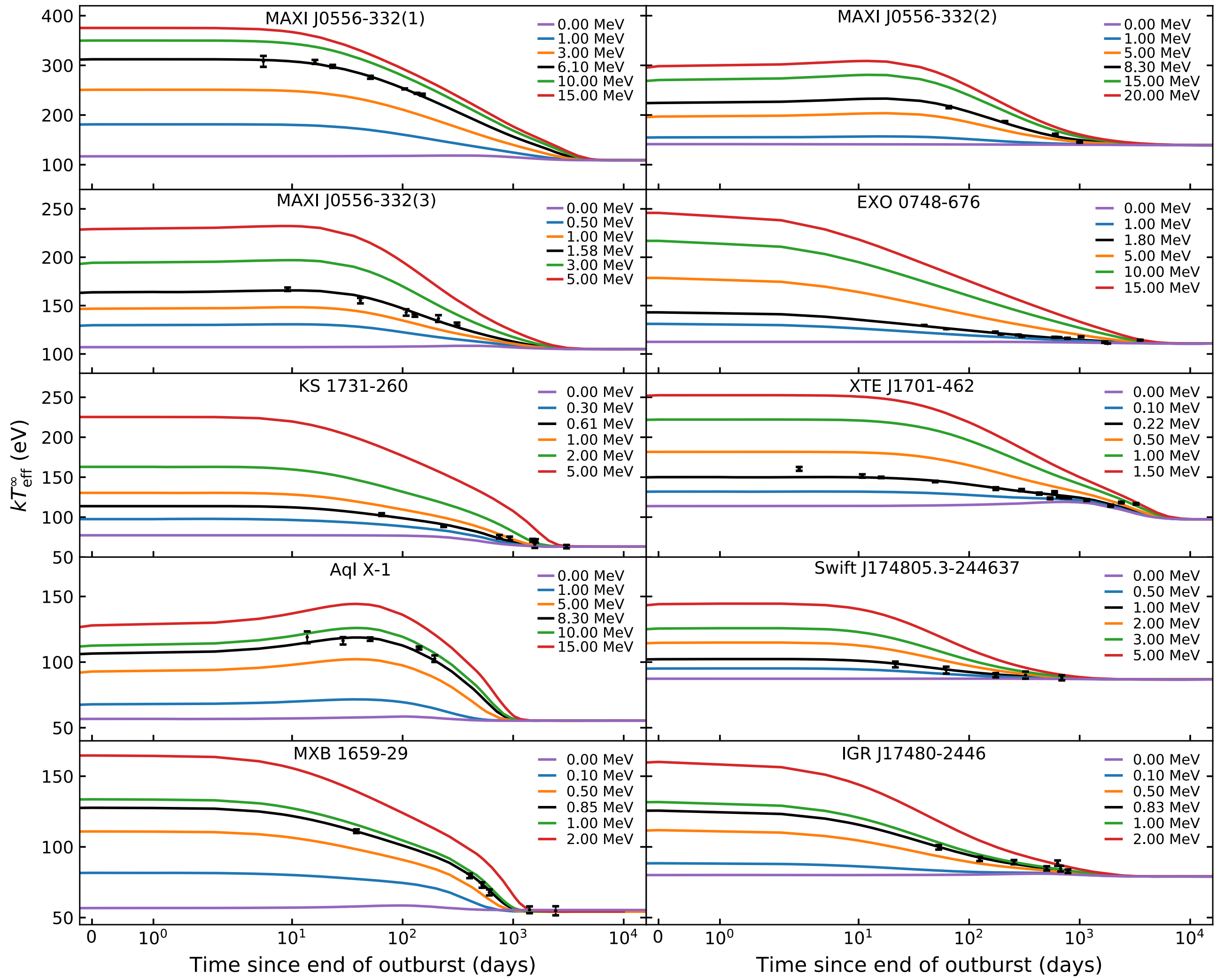

Figure 1. Model fit to the cooling curves with different magnitudes of shallow heat. The different colors represent the different magnitudes of shallow heat. The black lines in each panel represent the result of our fitting with observations, where the fitting parameters are shown in Table 2.

of shallow heat to fit the observational data of MXB 1659-29 after outburst I, and whether it is $\log p = 26.5$ or $\log p = 27.0$ or $\log p = 27.5$ where pressure p is in the unit of $\mathrm{erg\,cm^{-3}}$, it fits the observation well. This is because the cooling data are incomplete in the first few days after outburst. It is also similar for EXO 0748-676, KS 1731-260 and MAXI J0556-332(2). As a result, the observational data in the first few days after outburst are important to constrain the shallow heating.

3.3. Possibility of a Deeper Shallow Heating in Some Exceptional Sources

Having calculated the crustal cooling light curves with different magnitudes and depths of shallow heat in the above section, our finding is that the light curves are very sensitive to the magnitude and depth of shallow heat. So far, the crust cooling of 10 sources after outburst has been observed as shown in Table 1, and modeling the crust cooling of these sources needs an additional shallow heating in the crust. However, shallow heating was not found to be required in some cases. For example, the crust cooling light curves of Swift J174805.3-244637 can be adequately modeled using standard physics input, without the need to include an additional source of shallow heat. However, a heat source up to $\simeq$1.4 MeV nucleon^{-1} is still compatible with the observational data (Degenaar et al. 2015). The shallow heating for outburst II of MAXI J0556-332 could vary from $\sim$0 to 2.2 MeV nucleon^{-1} (Parikh et al. 2017a). It is currently unknown whether shallow heating occurs in all neutron stars, if so, the shallow heating should be deep in the crust for Swift J174805.3-244637 and MAXI J0556-332 during outburst II.

Besides the above cases, Rouco Escorial et al. (2019) studied the quiescent X-ray variability in the neutron star Be/X-ray transient GRO J1750-27, and proposed that the unheated crust

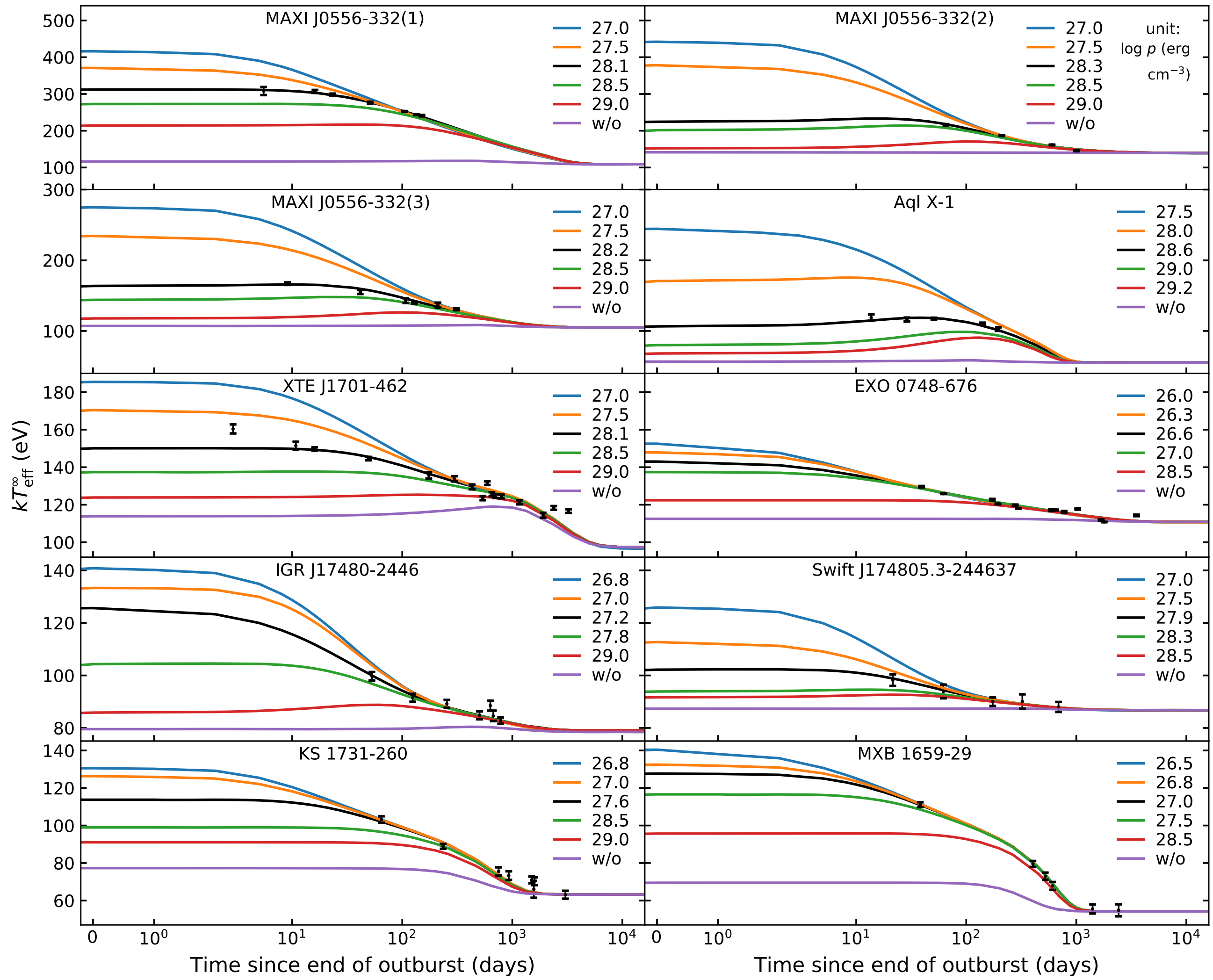

Figure 2. Model fit to the cooling curves with different depths of shallow heat. The different colors represent the different depths of shallow heat. The black lines in each panel represent the result of our fitting with observations, where the fitting parameters are shown in Table 2. The purple lines in each panel marked with "w/o" signify the case without shallow heating.

in GRO J1750 was caused by the shallow heating mechanism; the shallow heating process in GRO J1750-27 should be active at a much lower strength. As can be seen from Figure 2, if the shallow heat source is in a deep depth, there would be a plateau phase before the crust cooling. The deeper the heat source is, the longer the platform. Thus, it is possible that the heat source is in a deeper layer in GRO J1750-27. However, as GRO J1750-27 is a Be/X-ray transient, the temperature of the crust may also be affected by the magnetic field, though we do not consider it in this work.

Figure 3 shows the effective surface temperature as a function of shallow heating depth with the two representative sources MAXI J0556-332 and MXB 1659-29. When increasing the depth of shallow heating, the effective surface temperature overlaps in the first few days after outburst. The surface temperature will be the same in $\sim$100 days after outburst if the depth of shallow heating is deeper than $4.3 \times 10^{10}\,\mathrm{g\,cm^{-3}}$ for MXB 1659-29 after outburst I. While for MAXI J0556-332, the surface temperature will be consistent in $\sim$500 days after outburst if the depth of shallow heating is deeper than $1.8 \times 10^{11}\,\mathrm{g\,cm^{-3}}$. The difference between the two sources is caused by the accretion rate and the duration in active phase.

Figure 4 illustrates the evolution of the cooling layer by noting a given magnitude of shallow heating. The different lines in each panel represent the depth of shallow heating. The dots defining each curve indicate the maximum temperature during the evolution which prevents the crust cooling after outburst. In the inital days after outburst (e.g., $t = 50$ d, 100 d), the temperature is consistent in a large range from the surface to the deeper layers with increasing depth of the shallow

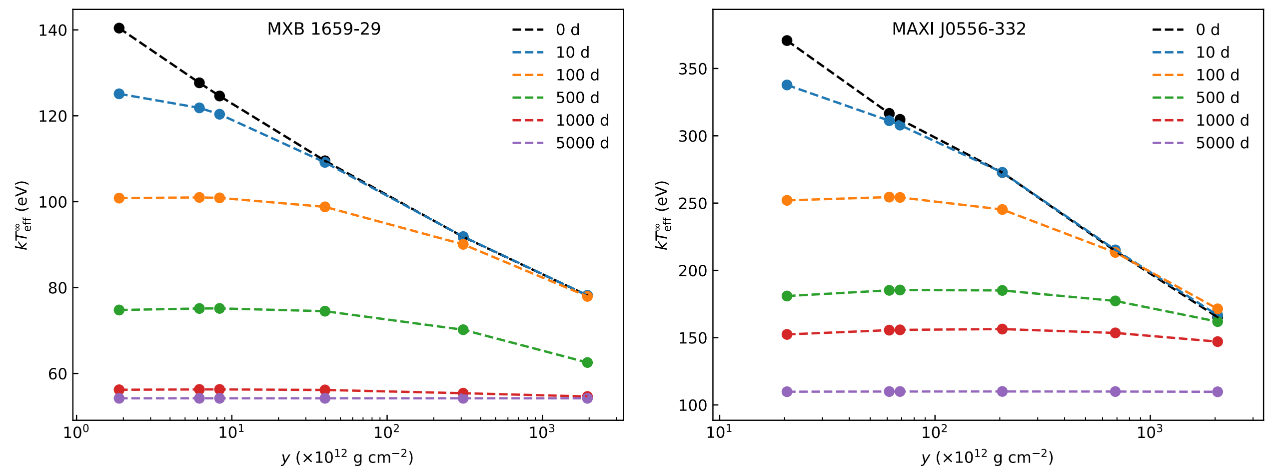

Figure 3. The effective surface temperature as a function of shallow heating depth. Different colors represent the different evolution times. Left: after the first outburst of MXB 1659-29. Right: after the first outburst of MAXI J0556-332.

Table 3
Shallow Heating Parameters ($Q_{\rm sh}$ and $\rho_{\rm sh}$) from NSCool and dStar for the Observed $kT_{\rm eff}^{\infty}$ Evolution in MXB 1659-29 and MAXI J0556-332 after Multiple Outbursts

	MXB 1659-29		MAXI J0556-332		
	Outburst I	II	Outburst I	II	III
NSCool $Q_{\rm sh}$ (MeV nucleon^{-1})	1.2 ± 0.8	$1.2^{+2.4}_{-0.7}$	$17.0^{+2.2}_{-0.7}$	2.2 ± 0.7	0.33 ± 0.03
$\rho_{\rm sh}$ ($\times 10^9$ g cm^{-3})	$0.4^{+8.8}_{*}$	$1.0^{+9.0}_{*}$	$5.3^{+0.2}_{-0.5}$	33.5 ± 0.8	1.6 ± 1.3
dStar $Q_{\rm sh}$ (MeV nucleon^{-1})	0.93	1.12	8.25	6.51	1.42
$\rho_{\rm sh}$ ($\times 10^9$ g cm^{-3})	1.8	1.3	15	23	14

Note. The NSCool data are taken from Table 2 of Parikh et al. (2017a) and Parikh et al. (2019). The dStar data are calculated from this work.

heating. In the late time evolution (e.g., $t \geqslant 500$ d), the crust gradually cools to the temperature of the core. We can further understand the inactive shallow heating behavior of some transiently accreting neutron stars by a much deeper shallow heating mechanism.

4. The Uncertainties of Shallow Heating

4.1. The Dependence of Shallow Heating Parameters on Crust Cooling Models

The values of shallow heating needed in Table 2 are different from those in the previous works. Here, we choose two representative sources MXB 1659-29 and MAXI J0556-332 for a detailed comparison with previous works, where the former needs small shallow heating as ∼1 MeV per accreted nucleon while the latter needs a large amount of shallow heating as 6–17 MeV per accreted nucleon to fit the quiescent light curve after first outburst.

Transient source MXB 1659-29 was discovered in 1976 (Lewin et al. 1976) and showed a ∼2–2.5 yr outburst (Wijnands et al. 2003). The second outburst from the source was detected in 1999 (in ’t Zand et al. 1999) that lasted ∼2.5 yr as well (Wijnands et al. 2002). This outburst is called outburst I because after it the crust cooling was studied. A new accretion outburst was detected in 2015 (Negoro et al. 2015); it lasted for ∼1.7 yr (Parikh et al. 2017b), which is referred to as outburst II. MAXI J0556-332 was discovered on 2011 January 11 (Matsumura et al. 2011) and showed a ∼16 month outburst. The second outburst of the source happened in 2012 which lasted ∼2 months (Sugizaki et al. 2012) and the third in 2016 lasted ∼3 months (Negoro et al. 2016).

Parikh et al. (2017a, 2019) studied the cooling of neutron star crusts in MXB 1659-29 and MAXI J0556-332 during different outbursts using the crust heating and cooling code NSCool (Page 2016). The shallow heating parameters of MXB 1659-29 and MAXI J0556-332 from NSCool can be found in Table 3. The first outburst in MXB 1659-29 was studied by Brown & Cumming (2009) and the first outburst in MAXI J0556-332 was examined by Deibel et al. (2015) with use of the thermal evolution code dStar (Brown 2015). The crust

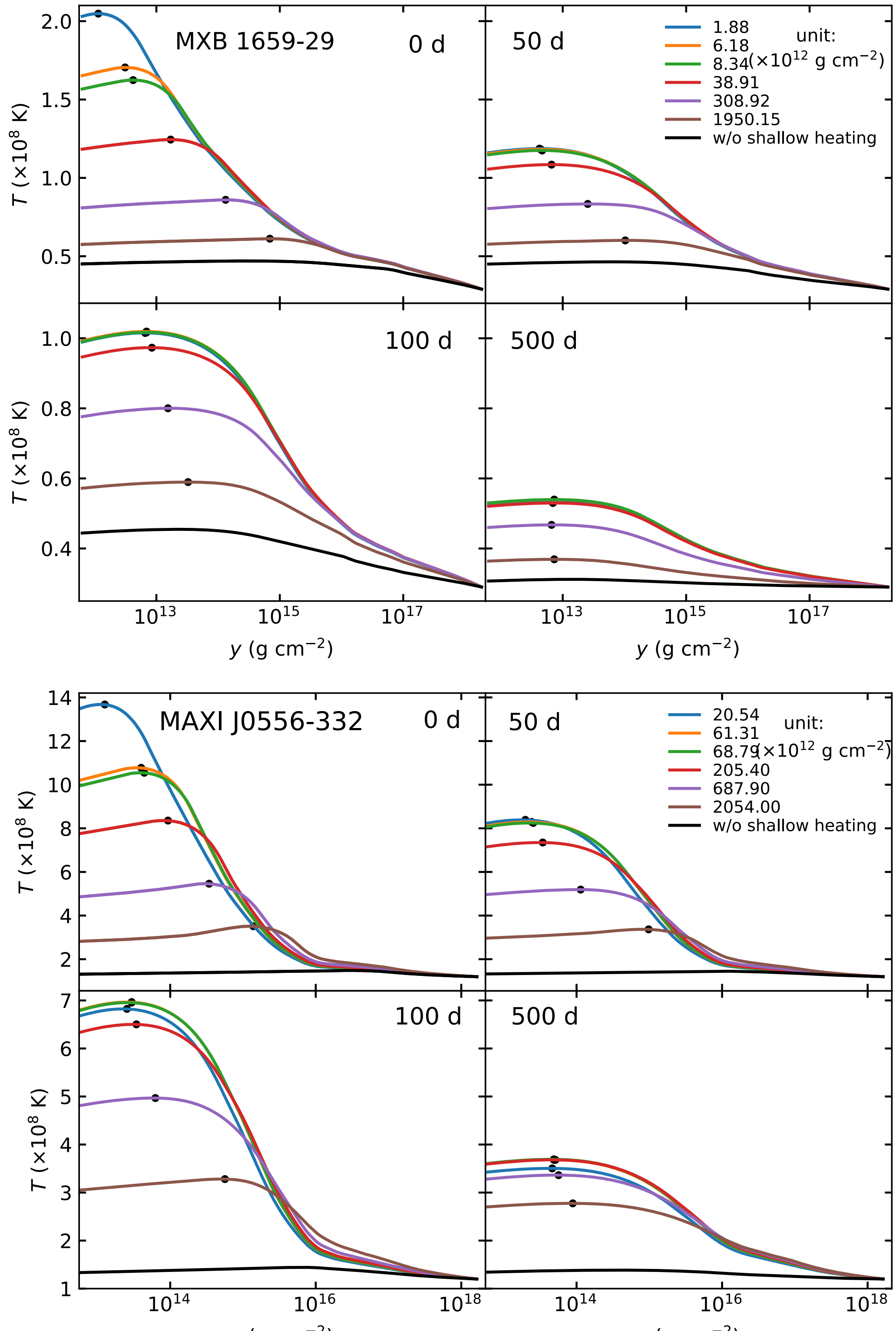

Figure 4. The temperature as a function of column depth y ($y \approx p/g$) at different days after outburst. The amount of shallow heat is fixed (0.85 MeV per accreted nucleon for MXB 1659-29 and 6.1 MeV per accreted nucleon for MAXI J0556-332). The depth of shallow heat is marked with different colors. The dots on each colored curve indicate the maximum temperature during the evolution. The black line indicates the case without shallow heating. Top: after first outburst of MXB 1659-29. Bottom: after first outburst of MAXI J0556-332.

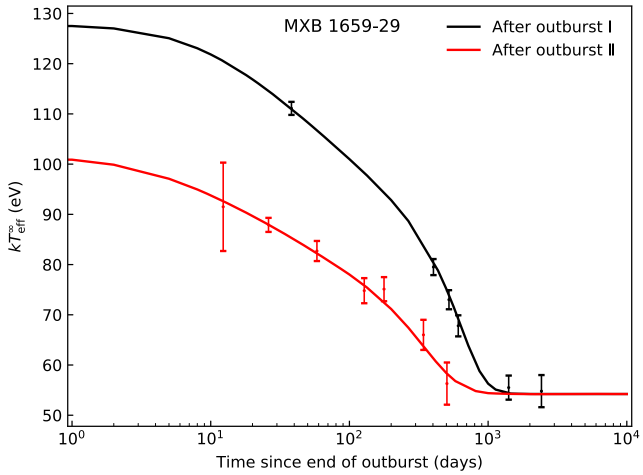

Figure 5. Model fit of the quiescent light curve after outbursts. The data after different outbursts are coded with color. Left panel: MXB 1659-29. Right panel: MAXI J0556-332.

cooling curves after their second or third outbursts are not studied with use of dStar. We calculate the crust cooling curves after multiple outbursts in MXB 1659-29 and MAXI J0556-332 using dStar in this work.

To compare the shallow heating parameters between dStar and NSCool codes, we adopt $M = 1.6\,M_{\odot}$ and $R = 12$ km neutron star accreting at $\dot{m} = 1.1 \times 10^{17}$ g s^{-1} for 2.5 yr for MXB 1659-29 during outburst I, and $\dot{m} = 5.7 \times 10^{16}$ g s^{-1} for 1.7 yr for outburst II which is the same as Model A of Parikh et al. (2019). We assume that an $M = 1.4M_{\odot}$ and $R = 10$ km neutron star accreted at $\dot{m} = 1.1 \times 10^{18}$ g s^{-1} for 16 months for MAXI J0556-332 during outburst I, $\dot{m} = 5.7 \times 10^{17}$ g s^{-1} for ∼2 months for outburst II and $\dot{m} = 7.7 \times 10^{16}$ g s^{-1} for ∼3 months for outburst III according to Parikh et al. (2017a). The additional model fit parameters were core temperature (T_c) and the impurity factor of the crust ($Q_{\rm imp}$). $T_{\rm c} = 3.1 \times 10^{7}$ K, $Q_{\rm imp} = 2.7$ for MXB 1659-29, and $T_{\rm c} = 5.9 \times 10^{7}$ K, $Q_{\rm imp} = 1$ for MAXI J0556-332 are adopted in this work. The column depth of light elements is set at $\sim y = 2.5 \times 10^{8}$ g cm^{-2} for MXB 1659-29 and $\sim y = 3 \times 10^{9}$ g cm^{-2} for MAXI J0556-332 which follow Parikh et al. (2019, 2017a). These parameters are a little different from Table 2.

In Figure 5, the quiescent light curves of MXB 1659-29 and MAXI J0556-332 after their multiple outbursts are fitted by using dStar. $Q_{\rm sh} = 0.93$ MeV nucleon^{-1} heat source is necessary to explain the quiescent light curve of MXB 1659-29 after outburst I and $Q_{\rm sh} = 1.12$ MeV nucleon^{-1} for outburst II, which are consistent with Brown & Cumming (2009) and Parikh et al. (2019). However, the depths of shallow heating are different between the two codes. While for MAXI J0556-332, both the magnitude and depth of shallow heating are different from those obtained from NSCool during the three outbursts. The detailed shallow heating parameters can be found in Table 2. The big difference of the shallow heating parameters between NSCool and dStar codes may be because a large amount of shallow heating is needed for MAXI J0556-332 while a small amount of shallow heating is needed for MXB 1659-29. On the other hand, the cooling code of NSCool solves the energy transport and conservation equations taking into account general relativistic effects (Page 2016), while dStar models the thermal evolution of the neutron star crust by solving the general relativistic heat diffusion equation using the MESA (Paxton et al. 2011, 2013, 2015) numerical libraries (Brown 2015). The difference in shallow heating parameters may come from the model itself and the uncertainties of free fitting parameters. Meanwhile, the microphysics inputs such as equation of state, envelope composition, neutrino cooling, superfluidity and thermal conductivities in the crust may lead to differences between the two models. For example, the bottom density of the envelope is set at $\rho = 10^{10}$ g cm^{-3} for dStar (Brown & Cumming 2009) while $\rho = 10^{8}$ g cm^{-3} for NSCool (Parikh et al. 2019). The nuclear heating deposited in the inner crust is 1.5 MeV/u, in the outer crust it is 0.2 MeV/u for dStar (Brown & Cumming 2009), while the nuclear heating is assumed to be 1.93 MeV/u in the inner crust for NSCool (Ootes et al. 2018).

4.2. The Dependence of Shallow Heating Parameters on Mass and Radius of Neutron Stars

We noticed that the mass and radius of a neutron star are different even for one source in different works. For example, Parikh et al. (2017a) adopted the mass and radius of neutron stars as 1.4 $M_{\odot}$ and 10 km respectively when fitting the crust cooling of MAXI J0556-332, while $M = 1.5$ $M_{\odot}$ and $R = 11$ km were adopted to fit the quiescent light curve of MAXI J0556-332 by Deibel et al. (2015). How do mass and

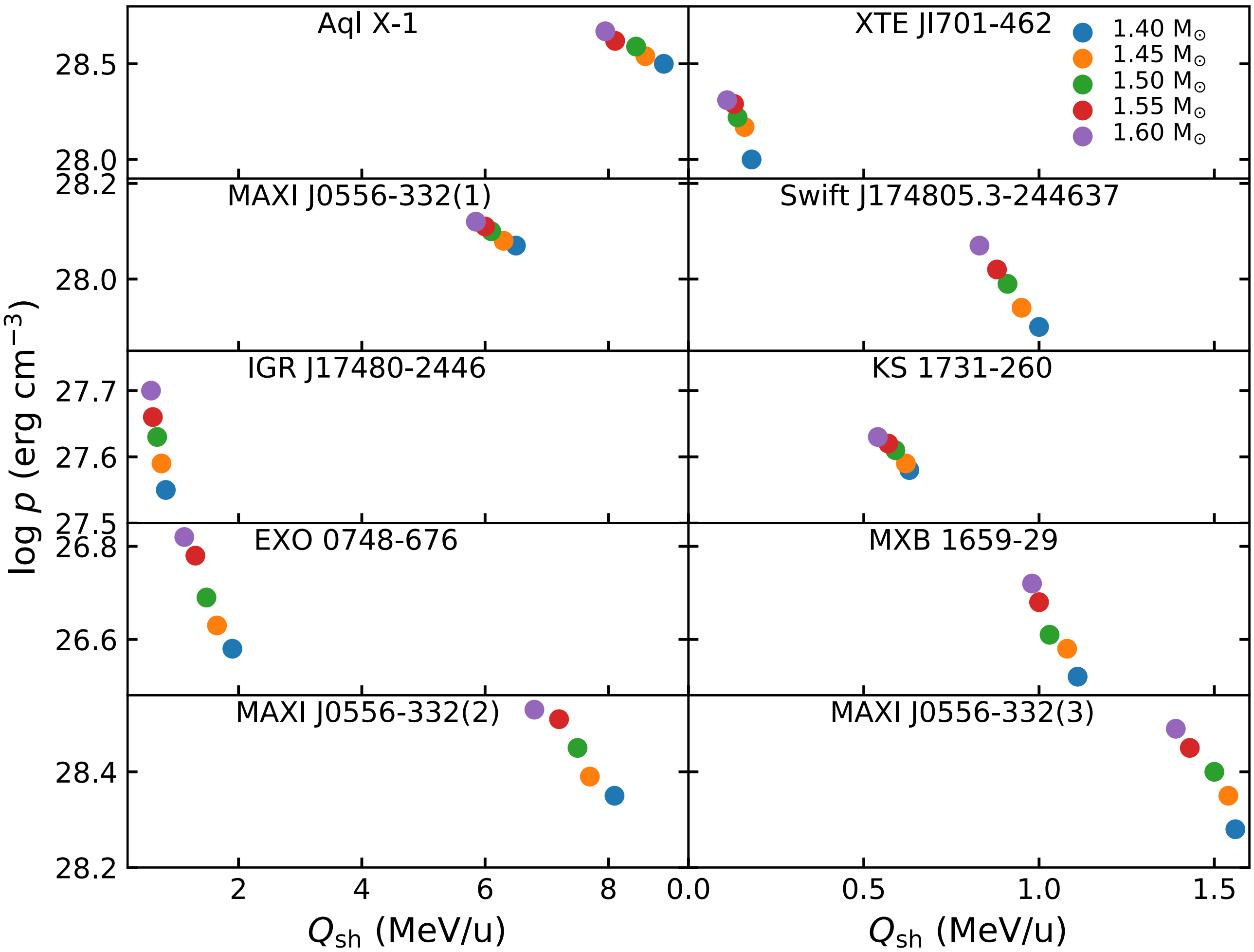

Figure 6. The constraint of shallow heating parameters (magnitude $Q_{\rm sh}$ and depth log p) with different neutron star masses (coded with different colors), where the radius is fixed at 11 km.

radius affect a neutron star in terms of shallow heating parameters? To answer this question, we fit the cooling curves of the eight sources which were studied in Section 3 with different masses and radii.

Figure 6 depicts our fitting parameters of shallow heating with different masses, where the radius is fixed at 11 km. We find that the shallow heating parameter is different for a different mass neutron star, and the more massive the neutron star, the smaller and deeper the shallow heat, and vice versa. The magnitude of shallow heating will reduce ∼10%–50% with increasing mass of the neutron star from 1.4 $M_\odot$–1.6 $M_\odot$ (e.g., for MAXI J0556-332(1), $Q_{\rm sh} = 6.5$ MeV/u with $M = 1.4$ $M_\odot$, $Q_{\rm sh} = 5.85$ MeV/u with $M = 1.6$ $M_\odot$, $Q_{\rm sh}$ reduced about ∼10% with increasing mass of neutron star from 1.4 $M_\odot$ to 1.6 $M_\odot$, while for XTE J1701-462, $Q_{\rm sh} = 0.17$ MeV/u with $M = 1.4$ $M_\odot$, $Q_{\rm sh} = 0.09$ MeV/u with $M = 1.6$ $M_\odot$, $Q_{\rm sh}$ reduced about ∼47% with increasing mass of neutron star from 1.4 $M_\odot$ to 1.6 $M_\odot$), which means the more compact the neutron star, the less shallow heating is required.

Figure 7 shows our fitting parameters of shallow heating with different radii, where the mass is fixed at 1.5 $M_\odot$. The radius also affects the shallow heating parameters. When increasing the radius of a neutron star, a bigger and shallower heat will be needed, and vice versa. The magnitude of shallow heating will increase ∼10%–40% with increasing radius of a neutron star from 10 km to 12 km, which means the less compact the neutron star, the more shallow heating is required. The results are consistent with the change of mass in Figure 6.

5. Conclusions

Comparing the crust cooling theory and observation of SXTs after an outburst is a unique way to study the properties of the crust of accreting neutron stars. In this paper, we have studied the crust cooling of eight sources (the multiple outbursts of

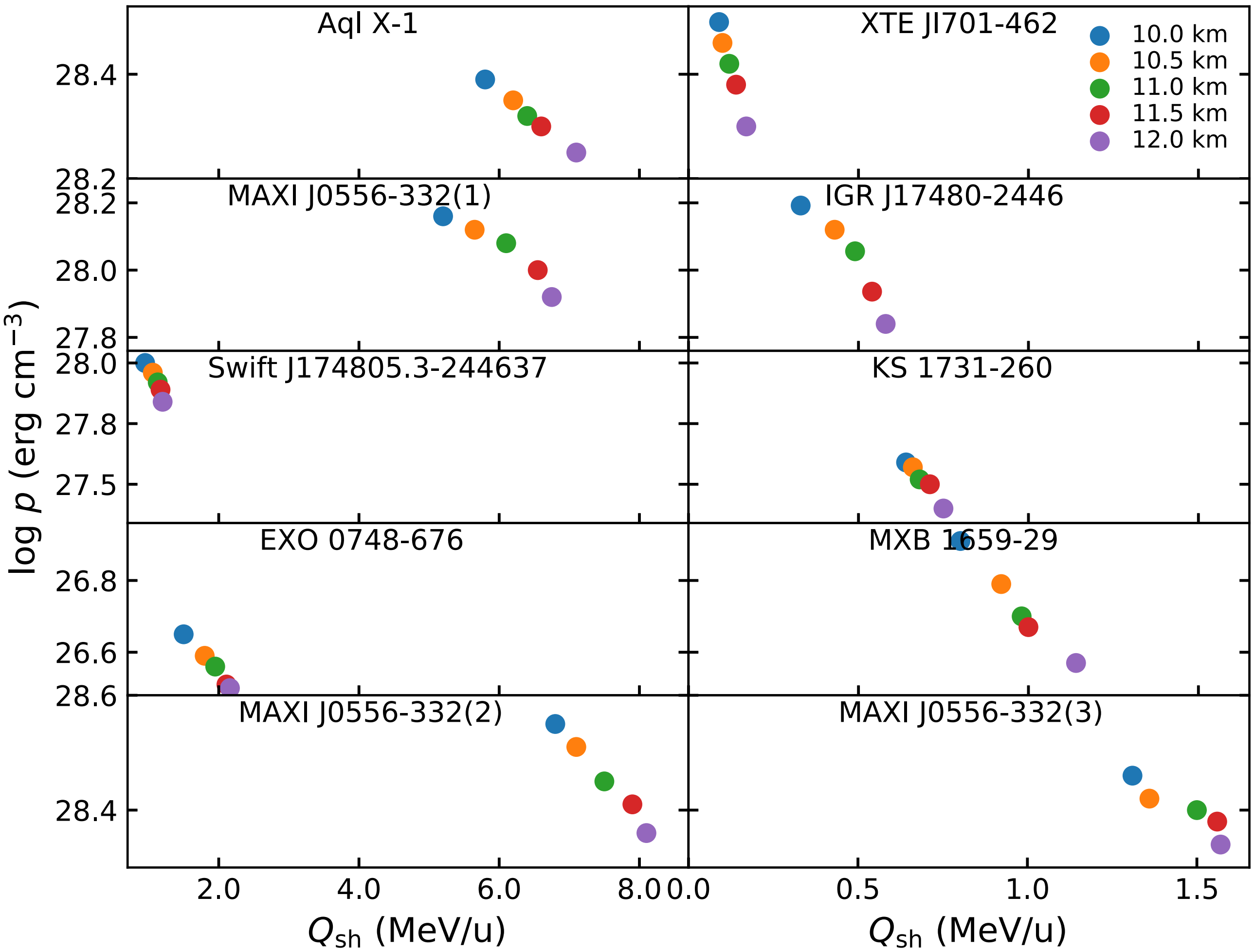

Figure 7. The constraint of shallow heating parameters (magnitude Q_{sh} and depth log p) with different neutron star radii (coded with different colors), where the mass is fixed as 1.5 $M_{\odot}$.

MXB 1659-29 and MAXI J0556-332 are also studied) with use of the public code dStar.

By using the fitting parameters of eight sources in Table 2, we study the effect of magnitude (Q_{sh}) and depth (ρ_{sh}) of shallow heating on the cooling curves. The results show that the shape of crust cooling curves is sensitive to Q_{sh} and ρ_{sh}. By fixing the depth of shallow heating, we change the amount of shallow heat and find that a large amount of shallow heat corresponds to a high crust temperature and a fast cooling rate, and vice versa. Similarly, when fixing the magnitude of shallow heating, we change the depth of shallow heat, and the results indicate that a shallow depth of the heat corresponds to a high crust temperature. When increasing the depth of shallow heating, there would be a plateau phase before the crust cooling. The conclusion implies that a small amount of shallow heat could lead to a heated crust and if the heat source is located at a shallow depth, a slow crust cooling will be observed. However, if the heat source is located in the deep layers in the crust, it will take time before crust cooling occurs, and the deeper the heat source, the longer the time, which would lead to the inactive shallow heating behavior of an accreting neutron star. Also, we find that the observations during the first days after outburst are important to decide the shallow heating parameters.

Based on our results, some exceptions such as Swift J174805.3-244637, outburst II of MAXI J0556-332, and GRO J1750-27 can possibly be explained by the shallow heating mechanism if there is a small shallow heat source in the deep layer in the crust of these neutron stars.

In addition, we find that the shallow heating parameters (Q_{sh} and ρ_{sh}) from dStar are different from those that were used in the NSCool code. The uncertainty of shallow heating parameters comes partly from the difference between models, and partly from the microphysics inputs of the crust. We investigate the effect of mass and radius of neutron stars on the shallow heating parameters. Both of them affect shallow heating parameters, and the more compact the neutron star, the less shallow heating will be needed.

As the origin of shallow heating is as yet unknown, the uncertainty of shallow heating could be constrained from crust cooling observations. The new observations on crust cooling of accreting neutron stars will hopefully produce more constraints on shallow heating parameters, which will help us to better understand shallow heating.

Acknowledgments

We would like to thank the anonymous referee for constructive comments that helped to improve the paper. This work has been supported by the Natural Science Foundation of Xinjiang Province under Grant No. 2020D01C063 and the National Natural Science Foundation of China (NSFC, Grant Nos. 11763007, U2031204 and 11863005).

References

Beznogov, M. V., Potekhin, A. Y., & Yakovlev, D. G. 2021, PhR, 919, 1
Brown, E. F. 2015, dStar: Neutron Star Thermal Evolution Code, (Astrophysics Source Code Library: ascl:1505.034)
Brown, E. F., Bildsten, L., & Rutledge, R. E. 1998, ApJL, 504, L95
Brown, E. F., & Cumming, A. 2009, ApJ, 698, 1020
Cackett, E. M., Wijnands, R., Linares, M., et al. 2006, MNRAS, 372, 479
Chamel, N., Fantina, A. F., Zdunik, J. L., & Haensel, P. 2020, PhRvC, 102, 015804
Degenaar, N., Medin, Z., Cumming, A., et al. 2014, ApJ, 791, 47
Degenaar, N., Ootes, L. S., Page, D., et al. 2019, MNRAS, 488, 4477
Degenaar, N., Ootes, L. S., Reynolds, M. T., Wijnands, R., & Page, D. 2017, MNRAS, 465, L10
Degenaar, N., Wijnands, R., Bahramian, A., et al. 2015, MNRAS, 451, 2071
Degenaar, N., Wijnands, R., Brown, E. F., et al. 2013, ApJ, 775, 48
Deibel, A., Cumming, A., Brown, E. F., & Page, D. 2015, ApJL, 809, L31
Haensel, P., & Zdunik, J. L. 1990, A&A, 227, 431
Haensel, P., & Zdunik, J. L. 2003, A&A, 404, L33
Haensel, P., & Zdunik, J. L. 2008, A&A, 480, 459
Han, S., & Steiner, A. W. 2017, PhRvC, 96, 035802
in 't Zand, J., Heise, J., Smith, M. J. S., et al. 1999, IAU Circ., 7138, 1
Lewin, W. H. G., Hoffman, J. A., Doty, J., & Liller, W. 1976, IAU Circ., 2994, 2
Liu, H., Dohi, A., Hashimoto, M.-A., et al. 2021a, PhRvD, 103, 063009
Liu, H.-L., Dai, Z.-G., Lü, G.-L., et al. 2021b, PhRvD, 104, 123004
Matsumura, T., Negoro, H., Suwa, F., et al. 2011, ATel, 3102, 1
Matsuo, Y., Liu, H., Hashimoto, M.-A., & Noda, T. 2018, IJMPE, 27, 1850067
Merritt, R. L., Cackett, E. M., Brown, E. F., et al. 2016, ApJ, 833, 186
Negoro, H., Furuya, K., Ueno, S., et al. 2015, ATel, 7943, 1
Negoro, H., Nakajima, M., Ueno, T. F. S., et al. 2016, ATel, 8513, 1
Ootes, L. S., Page, D., Wijnands, R., & Degenaar, N. 2016, MNRAS, 461, 4400
Ootes, L. S., Vats, S., Page, D., et al. 2019, MNRAS, 487, 1447
Ootes, L. S., Wijnands, R., Page, D., & Degenaar, N. 2018, MNRAS, 477, 2900
Page, D. 2016, NSCool: Neutron Star Cooling Code, (Astrophysics Source Code Library: ascl:1609.009)
Page, D., Homan, J., Nava-Callejas, M., et al. 2022, arXiv:2202.03962
Parikh, A. S., Homan, J., Wijnands, R., et al. 2017a, ApJL, 851, L28
Parikh, A., Wijnands, R., Bahramian, A., Degenaar, N., & Heinke, C. 2017b, ATel, 10169, 1
Parikh, A. S., Wijnands, R., Degenaar, N., Ootes, L., & Page, D. 2018, MNRAS, 476, 2230
Parikh, A. S., Wijnands, R., Homan, J., et al. 2020, A&A, 638, L2
Parikh, A. S., Wijnands, R., Ootes, L. S., et al. 2019, A&A, 624, A84
Paxton, B., Bildsten, L., Dotter, A., et al. 2011, ApJS, 192, 3
Paxton, B., Cantiello, M., Arras, P., et al. 2013, ApJS, 208, 4
Paxton, B., Marchant, P., Schwab, J., et al. 2015, ApJS, 220, 15
Potekhin, A. Y., & Chabrier, G. 2021, A&A, 645, A102
Rouco Escorial, A., Wijnands, R., Ootes, L. S., et al. 2019, A&A, 630, A105
Rutledge, R. E., Bildsten, L., Brown, E. F., et al. 2002, ApJ, 580, 413
Shchechilin, N. N., Gusakov, M. E., & Chugunov, A. I. 2021, MNRAS, 507, 3860
Sugizaki, M., Matsuoka, M., Negoro, H., et al. 2012, ATel, 4524, 1
Turlione, A., Aguilera, D. N., & Pons, J. A. 2015, A&A, 577, A5
Waterhouse, A. C., Degenaar, N., Wijnands, R., et al. 2016, MNRAS, 456, 4001
Wijnands, R., Degenaar, N., & Page, D. 2017, JApA, 38, 49
Wijnands, R., Muno, M. P., Miller, J. M., et al. 2002, ApJ, 566, 1060
Wijnands, R., Nowak, M., Miller, J. M., et al. 2003, ApJ, 594, 952
Wijngaarden, M. J. P., Ho, W. C. G., Chang, P., et al. 2020, MNRAS, 493, 4936
Yakovlev, D. G., Levenfish, K. P., & Haensel, P. 2003, A&A, 407, 265